Linear Free Energy Relationships. Part 10.[1] Synthesis, Thermal, Spectral, Electrochemical, and Hole Transport (Conduction) Properties of Some Novel Carbazole Derivatives

By **Harry W. Gibson,* George R. Olin,** and **John M. Pochan,** Webster Research Center, Xerox Corporation, 800 Phillips Road, Webster, New York, 14580, U.S.A.

A series of carbazole anils was prepared from 9-ethylcarbazole-3-carbaldehyde and 3-amino-9-ethylcarbazole. Thermal properties were examined by differential scanning calorimetry; most of the compounds form stable glasses and T_g/T_m values (average 0.75) are exceptionally high. The oxidation potentials of these compounds are not very sensitive to the substituent, except for the dimethylamino-case, where presumably oxidation of the amino-group itself occurs; the oxidations are generally irreversible. Hammett plots of the long-wavelength absorption energies have an inverted V shape with crossovers at σ *ca.* 0, as expected. Hole transport measurements reveal that in general the compounds derived from the carbazole carbaldehyde are superior to those derived from the aminocarbazole. This result is unexpected on the basis of the electrochemical results, in which the aminocarbazole derived compounds have lower oxidation potentials. This suggests that either the higher polarizability of the carbazolecarbaldehyde derived compounds, as reflected in their higher extinction coefficients, or less irreversible oxidation processes may be responsible for the better transport characteristics of the carbazolecarbaldehyde derived anils.

CARBAZOLE derivatives occupy a prominent position as basic active hole-transporting species in organic photoconductors.[2] Thus, polyvinylcarbazole and *N*-isopropylcarbazole have been extensively studied.[3,4] The present paper describes studies carried out on anil derivatives of *N*-ethylcarbazole in order to determine how the extended conjugation of these systems effects hole transport. Electrochemistry and spectroscopy have been used to relate the molecular orbital energetics to the transport characteristics. Thermal properties of the anils have also been examined as a measure of their tendency to form amorphous glasses, rather than to crystallize from polymeric matrices; this feature is important for the practical use of such molecules as solid solutions in polymeric matrices.[3-5]

RESULTS

A. *Synthesis.*—The synthesis of compounds of structure (1) involved condensation of 9-ethylcarbazole-3-carbaldehyde (3) and substituted anilines. Likewise, synthesis of series (2) proceeded from 3-amino-9-ethylcarbazole (4) and substituted benzaldehydes. These reactions are essentially quantitative. Formation of compounds of structure (2) proceeds more rapidly than formation of (1).

In addition to series (1) and (2), a number of related compounds were synthesized. Compound (5) was prepared in *ca.* 20% isolated yield (50% H_2O yield) from phenylenediamine and (3). Compound (6) was derived from (4) and terephthalaldehyde. Condensation of (3) and (4) yielded (7). Compound (8) resulted from reaction of (4) and pyrene-1-carbaldehyde. Reaction of polymer (9) [6] and (4) led to copolymer (10), *i.e. ca.* 80% conversion of aldehyde groups to anil groups. In all except the two instances mentioned above, yields were essentially theoretical. All the compounds are new. The m.p.s and elemental analytical data are presented in Table 1.

B. *Thermal Properties.*—In order to characterize the thermal properties of the pure compounds, differential scanning calorimetry (d.s.c.) was employed. Glass transitions could be observed for all but two of the compounds,

TABLE 1

Analytical data for carbazole anil derivatives

Compound	M.p.[a] (°C)	Calc. C (%)	Calc. H (%)	Calc. N (%)	Found C(%)	Found H (%)	Found N (%)
(1a)	*b*	84.7	7.4	7.9	84.3	7.85	7.85
(1b)	154.0—154.5 [c]	84.6	6.45	8.95	84.9	6.3	8.95
(1c)	*d*	84.6	6.45		84.0	6.3	
(1e)	182.6—183.6 [e]	76.0	4.85	8.45	75.85	5.1	8.45
(1f)	101.5—103.0 [e]	80.9	6.8		81.05	6.75	
(1g)	186.7—188.0 [f]	81.7	5.3	13.0	81.95	5.3	12.8
(2b)	117.0—118.0 [g]	84.6	6.45		84.5	6.5	
(2c)	95.5—96.5 [g]	84.6	6.45		84.55	6.45	
(2d)	167.5—168.0 [c]	73.45	5.0	12.25	73.45	4.95	12.25
(2e)	102.6—103.5 [g]	76.0	4.85	8.45	75.15	5.05	8.75
(2f)	133.5—135.0 [h]	80.9	6.8		81.3	6.75	
(2g)	145.0—146.0 [i]	81.7	5.3	13.0	81.5	5.25	13.1
(5)	234.0—235.0 [j]	83.35	5.85	10.8	83.25	6.0	10.8
(6)	232.0—233.0 [k]	83.35	5.85		83.25	5.3	
(7)	142.7—143.9 [c,l]	83.8	6.05	10.1	83.6	6.25	10.1
(8)	179.0—180.0 [e]	88.1	5.25		87.9	5.3	
(10)	*m*	82.7	6.75	5.7	82.5	6.2	6.2

[a] In open capillaries using Thomas–Hoover apparatus, corrected. [b] B.p. 225° at 8 × 10^{-5} mmHg. [c] Recrystallized from benzene. [d] B.p. 223° at 1.9 × 10^{-5} mmHg. [e] Recrystallized from methanol. [f] Recrystallized from toluene. [g] Recrystallized from ethanol. [h] Recrystallized from ethanol–benzene. [i] Recrystallized from ethanol–toluene. [j] Recrystallized from tetrahydrofuran. [k] Recrystallized from dioxan. [l] M.p. is after washing with hexane or ethanol. Needles as formed from benzene, m.p. 80—87°, then re-solidify. [m] Purified by four precipitations from tetrahydrofuran solutions into rapidly stirred ethanol.

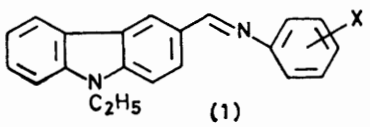

(1)

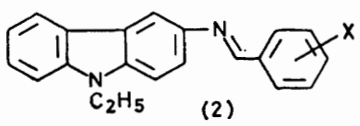

(2)

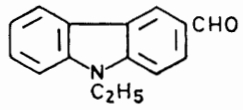

(3)

a; X = *p*-(n-C_4H_9) e; X = *p*-Cl
b; X = *p*-CH_3 f; X = *p*-$N(CH_3)_2$
c; X = *m*-CH_3 g; X = *p*-CN
d; X = *p*-NO_2

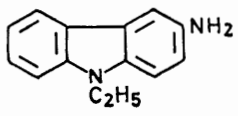

(4)

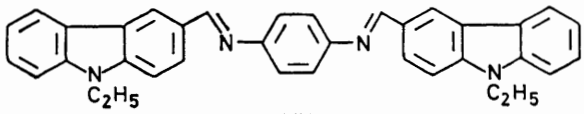

(5)

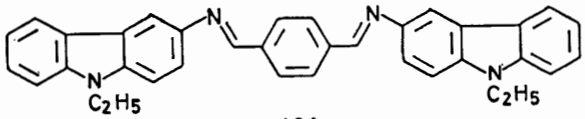

(6)

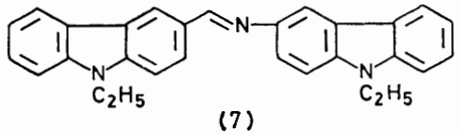

(7)

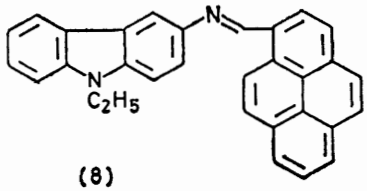

(8)

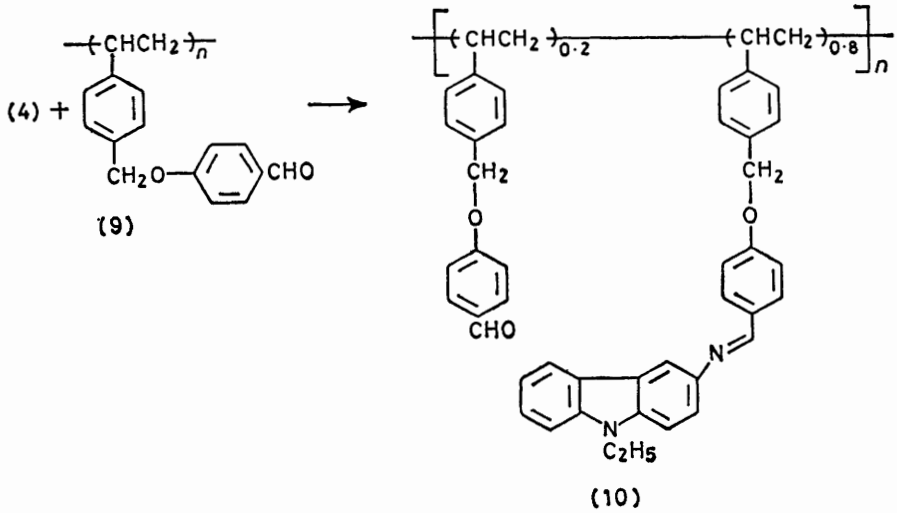

(9)

(10)

even though all but (10) are monomeric. The thermal data are presented in Table 2. Enthalpies and entropies of fusion were also determined as indicated.

TABLE 2

Thermal data [a] for carbazole anil derivatives

Compound	T_m/K	T_g/K	T_g/T_m	ΔH_t [b]/kcal mol^{-1}	ΔS_t [c]/cal mol^{-1} K^{-1}
(1a)		265			
(1b)	431	298	0.691	4.09	9.49
(1c)	*d*	275			
(1e)	455	293	0.644	9.29	20.4
(1f)	378	315	0.833	5.71	15.1
(1g)	463	320	0.691	8.56	18.5
(2b)	394	295	0.749	5.90	15.0
(2c)	372	285	0.766	4.87	13.1
(2d)	445	*e*		8.37	18.8
(2e)	376	293	0.779	5.28	14.0
(2f)	413	320	0.775	5.66	13.7
(2g)	420	307	0.731	6.49	15.5
(5)	511			5.66	11.1
(6)	508	359	0.707	12.4	24.4
(7)	418	350	0.837	5.41	12.9
(8)	456	348	0.763	9.40	16.2
(10)		410			

[a] Obtained at scan rate of 10° min^{-1} using Perkin-Elmer DSC-II. Temperature calibrated with standards, enthalpy with pure indium metal. T_m taken as maximum in transition. T_g taken as midpoint of C_p change. [b] Estimated precision 0.1—0.3 kcal mol^{-1}. [c] Estimated precision 0.2—0.7 kcal mol^{-1}. [d] Sample partially crystallized upon standing for several months. [e] Not observed but melt recrystallizes reproducibly at 340° when cooled, perhaps indicative of incipient T_g.

C. *Electronic Spectra.*—U.v.–visible spectra of all the soluble carbazole anils were recorded in order to ascertain the effects of changes in molecular structure upon electronic transitions. The results are given in Table 3.

TABLE 3

Spectral data for carbazole anil derivatives [a]

Compound	$\lambda_{max.}$/nm	$E = h\nu$/eV	$10^{-4}\epsilon$/mol l^{-1} cm^{-1}
(1a)	336	3.69	2.93
(1b)	336	3.69	3.44
(1c)	333	3.72	2.83
(1e)	338	3.67	3.36
(1f)	378	3.28	3.49
(1g)	348, 360 [b]	3.56, 3.44 [b]	3.41, 3.26 [b]
(2b)	346	3.58	2.09
(2c)	347, 354 [b]	3.57, 3.50 [b]	1.93, 1.89 [b]
(2d)	412	3.01	2.02
(2e)	358, 368 [b]	3.46, 3.37 [b]	1.77, 1.85 [b]
(2f)	357, 370 [b]	3.47, 3.35 [b]	4.44, 4.12
(2g)	387	3.20	2.03
(7)	348, 369 [b]	3.56, 3.36 [b]	3.21, 2.67 [b]
(8)	405	3.06	3.61

[a] In acetonitrile, *ca.* 5 × 10^{-4}M. [b] Shoulder.

D. *Electrochemical Oxidation Potentials.*—To attempt to understand the relationship of molecular structure and molecular orbital energy levels and electrical properties, solution-phase oxidation potentials of all the soluble members of these series of compounds were determined. These are collected in Table 4.

E. *Photoinduced Discharge (PIDC) Method as a Measure of Charge Transport.*—A representation of a PIDC experiment is shown in Figure 1.[7] Photodischarge is a two-step process, charge generation and discharge. These samples are made so that the photogeneration step takes place in the 0.5 μ amorphous selenium layer on which the sample is

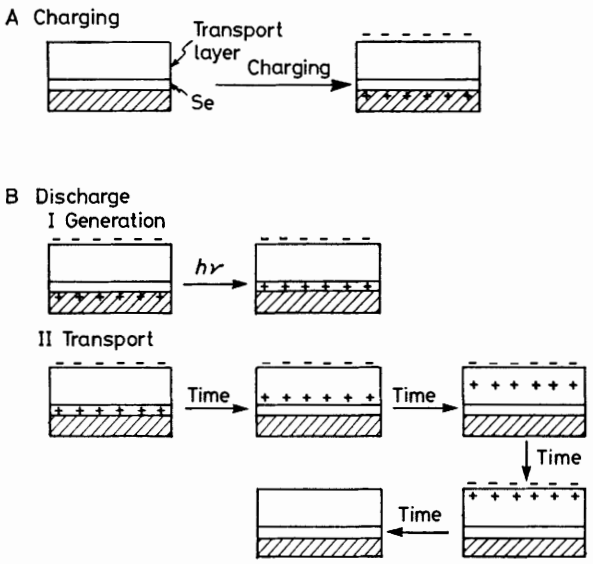

FIGURE 1 Representation of photoinduced discharge method of measuring positive charge ('hole') transport (conductivity)

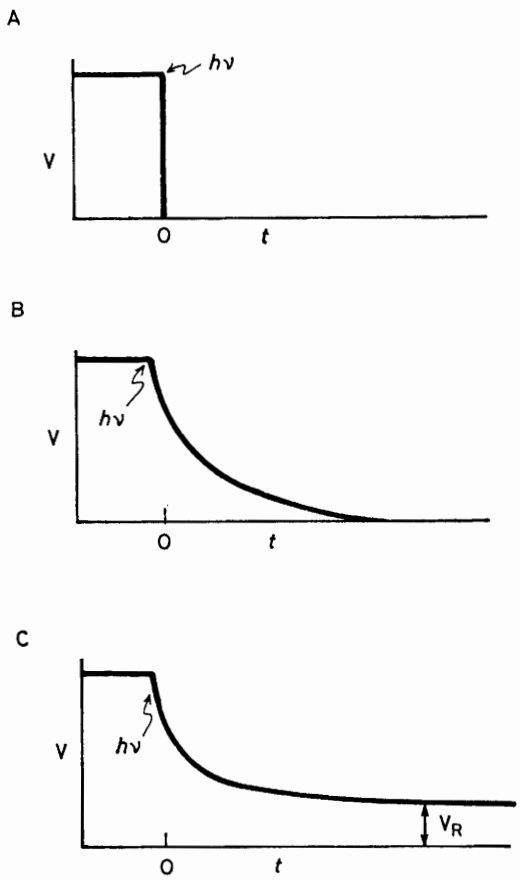

FIGURE 2 Voltage–time curves for various photoinduced discharge situations: A, ideal surface voltage–time curve; B, voltage-time curve for non-ideal system with no trap limitations; C, voltage–time curve for a non-ideal system with trap limitations

coated. The wavelength of the excitation light is chosen so that little if any radiation is absorbed in the organic layer. The sample is initially corona-charged to its capacitive limit (Figure 1A). A short-pulse strobe light is then applied at an appropriate wavelength such that hole-electron pairs are formed in the selenium layer (Figure 1B). Many of the electrons generated in the selenium layer then combine with holes in the backing conductive layer, thus leaving the remaining holes in the selenium to migrate to the surface of the sample and recombine with the surface electrons to reduce the surface charge to zero. If the surface voltage of the sample were monitored as a function of time, the discharge would look like that in Figure 2. There are, however, defects in the bulk of the material that cause the charges to move through the sample at varying velocities. This causes the arrival times at the surface of the sample to be different and the discharge appears as in Figure 2B.[4,5,8] An additional complication is permanent charge traps in the sample which limit the amount of charge that can be transported. In that case a residual in the PIDC voltage (V_R) (Figure 2C) is observed. If there are sufficient traps the sample will not discharge. If the velocity of the charges is high enough and trapping limitations do not occur, and the time between light flash and arrival of the charges at the surface of the material can be measured, the mobility ($\mu = V/E$) can be calculated. V = velocity = sample thickness divided by the transit time and E = electric field = voltage across the sample divided by the sample thickness.[4,5,8] In our experiments trap limitations did not permit a mobility analysis.

DISCUSSION

A. *Thermal Properties.*—The most striking feature of the thermal data is the large variation brought about by small changes in molecular structure. For example, in series (1) T_m varies from below room temperature to 463 K, T_g from 265 to 320 K, T_g/T_m from 0.644 to 0.833, and ΔH_f from 4.09 to 9.29 kcal mol^{-1}. These changes result from changing a single substituent, X. Similar changes take place in series (2) (see Table 2).

Perhaps the only definitive statement that can be made at this point in the absence of knowledge of the crystal structures is that these large changes in thermal properties are not well correlated in general by molecular structures. However, a few points of interest do emerge from consideration of the data. First, in series (2), ΔH_f and ΔS_f are relatively insensitive to the nature of the X group except where X = CN or NO_2 (2g and d). It is tempting to ascribe this to the formation of some sort of a ' charge transfer ' solid-state structure for the latter two compounds but not the others. Secondly, the T_g values of the analogous members of series (1) and (2) [*e.g.* (1b) and (2b)] are very similar. Thirdly, while T_m values for (5) and (6) are very similar, ΔH_f and ΔS_f for (6) are more than twice those for (5). In fact, (6) has the highest values of all the compounds studied.

It is noteworthy that all but two of the sixteen monomeric anil compounds form glasses near room temperature. The T_g/T_m ratios are also exceptional in being so high (average 0.747). For monomeric compounds T_g/T_m is reported to vary from 0.39 to 0.75; most are less than 0.7.[9] In the cases of (1f) and (7) the present values (0.833 and 0.837) are therefore exceptional. Compounds (1f) and (7) are also very similar from a molecular viewpoint in that both contain unit (A).

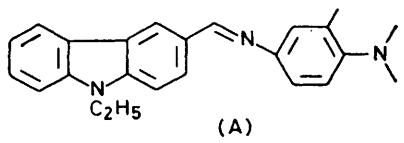

(A)

Many of these glasses are quite stable to crystallization at room temperature, presumably because T_g is above room temperature and hence there is little molecular mobility.

B. *Electronic Spectra.*—A plot of the electronic transition energies at the maximum absorbance (not shoulder) for series (1) and (2) anils (Table 3) *versus* Hammett substituent constants is given in Figure 3. Note that for both series inverted V-shaped plots are obtained. The crossover from one wing of the V to the other occurs at σ *ca.* 0 (X = H) in both cases. The shapes and $\sigma = 0$ crossover are typical of Hammett plots for electronic transition energies of substituted benzene systems.[10]

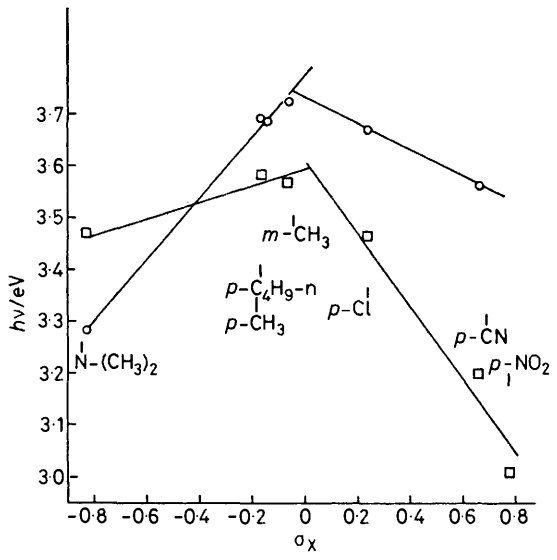

FIGURE 3 Long-wavelength transition energies as a function of Hammett substituent constants: ○, series (1); □, series (2)

It is noteworthy that the extinction coefficients for series (1) are generally greater than those of series (2). As seen in Figure 4, the only exception is the $N(CH_3)_2$ substituent. In fact, a fairly linear relationship exists for $\sigma < 0.23$. Since the extinction coefficient is a measure of the polarizability of the π-electrons, this indicates that the polarizabilities of series (1) are larger in general than those of series (2). This is most likely due to the fact that the $-CH=N-R$ linkage is more electron-withdrawing than the $-N=CHR$ linkage (see section C below), thus resulting in greater charge separation in (1) than in (2).

C. *Oxidation Potentials.*—The oxidation potentials of Table 4 are plotted against the electrophilic substituent

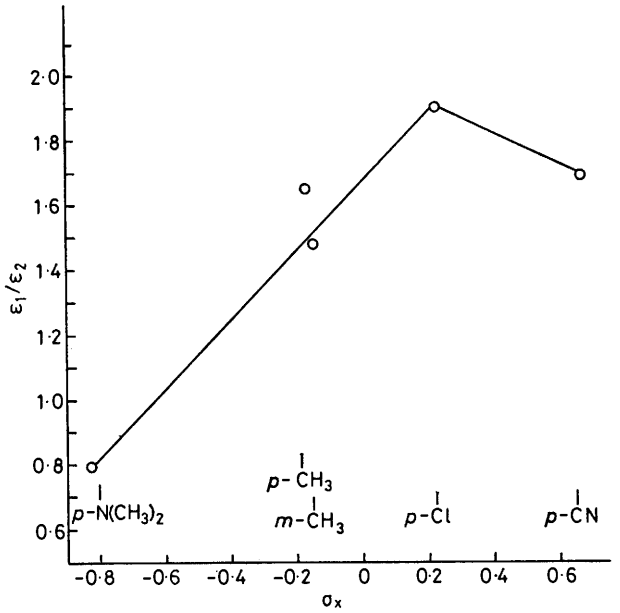

FIGURE 4 Ratio of extinction coefficients of lowest energy electronic transitions of series (1) to series (2) *versus* Hammett substituent constants

constants [11] in Figure 5. For each series the data fit a straight line of modest slope with one point [X = N-$(CH_3)_2$] deviant. Such deviations are not unknown for this substituent [12] and may be ascribed to loss of an

TABLE 4

Oxidation potentials of carbazole anil derivatives [a]

Compound	$E_{p/2}^{ox}$/V [b]	Reversibility [c]
(1a)	1.31	—
(1b)	1.30	—
(1c)	1.33	—
(1e)	1.31	—
(1f)	0.72,[d] 0.98, 1.26	+, —, —
(1g)	1.34	—
(2b)	1.09	—
(2c)	1.09	—
(2d)	1.12	—
(2e)	1.08	—
(2f)	0.79	—
(2g)	1.14	—
(7)	0.96	—
(8)	0.95	—

[a] *ca.* 5×10^{-4}M in acetonitrile, with 0.1M-tetrabutylammonium fluoride electrolyte using Princeton Applied Research model 170 system with s.c.e. reference and Pt button working and Pt auxiliary electrodes in cyclic voltammetric mode at 200 mV s^{-1} scan rate. [b] V *versus* s.c.e. at half-peak height. [c] + = reversible; — = irreversible. [d] $(E_{pa}^{ox} + E_{pc}^{ox})/2$.

electron from the *n*-orbitals of the substituent itself rather than from the π-electron system. An oxidation (the third observed) at a potential of 1.26 V was observed for (1f) [X = $N(CH_3)_2$] and this point falls on the straight line describing the rest of the data and may be due to π-oxidation.

As argued above, the -CH=N-R [series (1)] moiety is more electron-withdrawing than the -N=CHR moiety [series (2)] as evidenced by the lower oxidation potentials of series (2) relative to series (1). This is also borne out in the cases of (1f) and (2f) for which the localized oxidation of the $N(CH_3)_2$ group is facilitated more by the -N=CH-R moiety in series (1) than by the -CH=NR moiety of series (2). Moreover, as expected, with the exception of the dimethylamino-compounds the oxidation potentials of series (1) are higher than that of 9-ethylcarbazole ($E_{p/2}^{ox}$ 1.12 V [13]) while those of series (2) are lower.

As observed with other arylamines [14] oxidation of these compounds is generally irreversible; the only exception is (1f) [X = $N(CH_3)_2$]. Presumably as in other arylamines [14] this is due to radical cation coupling to yield

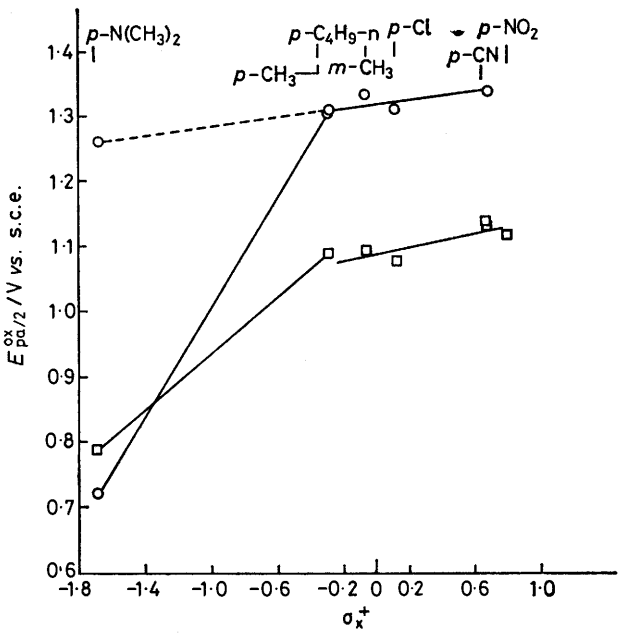

FIGURE 5 Oxidation potentials as a function of electrophilic substituent constants: ○, series (1); □, series (2)

bis(carbazoles) linked at the 6-positions. The mode of oxidation is not clear, however. The oxidation might be centred on the carbazole moiety, the case upon which the above arguments are based, or it might be centred upon the anil linkage.[12]

D. *Hole Transport* via *Photoinduced Discharge Analysis.*—Two problems occurred in the attempts to measure mobilities in the monomer systems. First, many of the monomer materials would not form stable solid solutions at 30% loading in the polycarbonate matrix. Measurements at lower loading levels indicated high charge trapping or extreme mobility limitations such that the samples could not be discharged on a reasonable time scale. Because of this, the following discussion is limited to a qualitative comparison of compounds (1b), (1e—g), (2b—d), (2f), (2g), (7), (8), and (10). Sample (10), the polymer, was studied in the pure phase.

A qualitative ranking of all samples tested *via* the PIDC method in terms of initial discharge rate and

amount of charge dissipated is as follows: (1f), (2f), (7), (1g), (1e) > (1b) ≈ (2c) ≫ (8), (2b), (2g, (2d), (10) (no transport in this last group). A more quantitative comparison of the five materials that exhibit the best discharge characteristics is not possible with the data in hand.

Comparative PIDC curves for the isomers (1f) and (2f) are given in Figure 6. The data shown are for measurements of hole transport. These materials show no evidence of electron transport. It is seen that (1f) and (2f) provide very similar discharge curves. The initial discharge rate of sample (2f) is higher than that of (1f), but it would be difficult to assign these differences to the

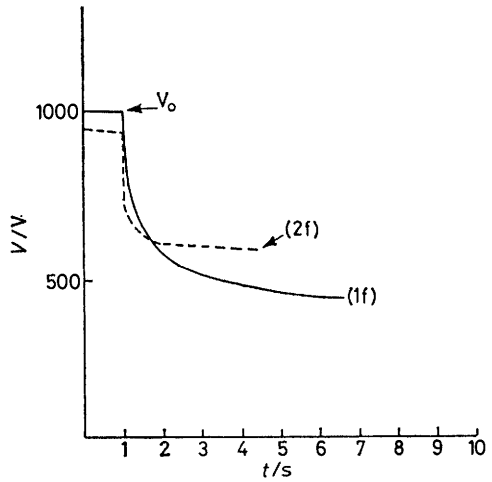

FIGURE 6 Photoinduced discharge curves for compounds (1f) and (2f) in polycarbonate

chemical structure as subtle differences in solubility of the compounds as well as their aggregative properties could cause these differences. Both samples exhibit large residual voltages which can be reduced by additional white light pulses, an indication that trapping of charge is occurring in the bulk.[2,7] Trapping is generally associated with molecular species whose radical cation state is lower in energy than the majority of charge carriers.[8] The bis(carbazoles) formed by coupling of the initially formed radical cations leads to species with lower ionization potentials.[14] Thus, the lower residual voltage observed with (1f) may be due to the fact that its first oxidation is reversible, while that of (2f) is not and leads to dimeric structures of lower oxidation potential. In agreement with this is the fact that while the oxidation potentials of (1e and g) are similar (Table 4), the residual voltage for (1g) is much higher than that of (1e) ($V_R/V_0 = 0.70$ and 0.45 at 13 s, respectively). The oxidation of (1g) appears qualitatively less reversible than that of (1e). Repeated voltammetric scans of most of the samples revealed the presence of material with 0.1—0.3 V lower oxidation potential than the starting anils.

The lack of detectable hole transport in (2b, d, and g) is most likely due to the low degree of polarizability as deduced from the low extinction coefficients (see Table 3 and Figure 4) or a more irreversible oxidation process, which negates the more favourable, lower oxidation potentials [2] in series (2) relative to series (1). In fact, the discharge rates for compounds (1) are all higher than those for corresponding compounds (2). This is taken as evidence that either the polarizability or the extent of reversibility or both factors is/are the determining factor(s).

It is interesting that the pyrene-substituted compound (8) exhibits no transporting characteristics even though a large electron-donating group is attached and pyrene derivatives are generally good transport materials.[2,15]

Williams and Limburg have shown that in polymers based on carbazole, overlap of the carbazole group is essential in obtaining high charge carrier (hole) mobilities.[16] In polymer (10) the carbazole groups are far from the polymer backbone so that overlap will not be forced by the polymer. Thus, the inability of the polymer to conduct holes is not unexpected.

Conclusions.—A number of anils derived from 9-ethylcarbazole-3-carbaldehyde and 3-amino-3-ethylcarbazole have been synthesized and characterized by d.s.c., electronic spectroscopy, electrochemical oxidation, and hole transport (conduction) measurements. These compounds show a tendency to form stable glasses with high T_g/T_m values (average 0.75). The hole conductivity of the anils derived from the carbazole-aldehyde is greater in spite of the fact that their oxidation potentials are higher than those of the anils derived from the aminocarbazole. This is attributed to either the lower polarizability of the latter series, as deduced from lower extinction coefficients for electronic excitation, or a more irreversible oxidation process, which can lead to dimers that function as hole traps, or a combination of the two factors.

EXPERIMENTAL

General.—Elemental analyses were carried out by Spang Laboratories, Eagle Harbor, Michigan. Except where noted, all starting materials were commercial products used as received.

9-Ethylcarbazole-3-carbaldehyde (3).—The compound received from Aldrich was purified by the following method. A column $1\frac{1}{2} \times 7\frac{1}{2}$ in was prepared from a slurry of Woelm neutral alumina (175 g). Compound (3) (101 g) was applied in toluene (200 ml) and eluted with toluene (1 l). The solvent was removed from the eluant and the residue was washed in a blender with n-hexane (250 ml) to afford (3) (90 g) as a pale yellow solid, m.p. 85.5—87.5°.

3-Amino-9-ethylcarbazole (4).—This compound was purchased from Aldrich who claimed it to be 90% pure. Attempts to purify the brown solid by recrystallization and column chromatography were unsuccessful.

Carbazole Anils.—The following general procedure was applied to the synthesis of the title compounds. A solution of the aldehyde (0.100 equiv.), the amine (0.100 equiv.), and dry benzene (100 ml) was heated under reflux under Drierite protection using a Dean–Stark trap for 18 h. However, in the case of reactions of aminocarbazole (5) reactions were usually complete in less time (2—3 h). Some

or all of the benzene was distilled to yield the product, which was purified by either distillation or recrystallization. In the case of (5) only 50% of the theoretical water production was observed in 18 h and none in a subsequent 7 h, so the reaction solution was concentrated and poured through a short (4 in) column of Woelm neutral alumina. Recrystallization of the solid resulting from this treatment afforded pure (5). Solvents and m.p.s are given in Table 1.

Thermal Properties.—Differential scanning calorimetric data was taken with a Perkin-Elmer DSC-II instrument at a scanning rate of 10° min^{-1}. Results are gathered in Table 2.

Electron Spectra.—Electronic spectra were obtained using a Cary 17D instrument and scanning downward from 800 nm. Table 3 summarizes the results.

Oxidation Potentials.—Oxidation potentials were determined in dry acetonitrile containing *ca.* 5×10^{-4}M-carbazole anil and 0.1M-tetrabutylammonium fluoroborate using a Princeton Applied Research model 170 system with standard calomel reference electrode, a platinum button working electrode, and a platinum auxiliary electrode. Experiments were generally performed in the cyclic voltammetric mode at 200 mV s^{-1} scan rate; some scans were done at 500 mV s^{-1} to test reversibility. Results are given in Table 4.

Photoinduced Discharge Charge Transport Measurement.—Transport measurements were made by the PIDC method of analysis.[7] Samples were prepared by casting 10 wt. % (g ml^{-1}) CH_2Cl_2 solutions of the monomer materials in polycarbonate (M_n 10 600, molecular weight distribution 2.5). The solid concentrations of the films were 30 wt. % monomer and 70 wt. % polycarbonate. The solutions were cast over a 0.5 μ layer of amorphous selenium coated on ball-grained aluminium. After casting, the films were dried *in vacuo* (10^{-4} mmHg) at ambient temperature for five days. The samples were tested for hole and electron transporting capability by corona charging positively or negatively and exposing the charged sample to a short strobe pulse of filtered light (433 nm) and monitoring the surface charge of the sample as a function of time. Complete details of the measurement are explained in ref. 7.

[1/128 *Received*, 28*th January*, 1981]

REFERENCES

[1] Part 9, H. W. Gibson and F. C. Bailey, *Chem. Phys. Lett.*, 1975, **51**, 352; Part 8, H. W. Gibson, *Can. J. Chem.*, 1977, **55**, 2637.

[2] M. Stolka and D. M. Pai, *Adv. Polym. Sci.*, 1978, **29**, 1; J. M. Pearson, *Pure Appl. Chem.*, 1977, **49**, 463.

[3] H. Hoegl, *J. Phys. Chem.*, 1965, **69**, 755.

[4] J. Mort, G. Pfister, and S. Grammatica, *Solid State Commun.*, 1976, **18**, 693.

[5] W. Limburg, D. M. Pai, J. M. Pearson, D. Renfer, M. Stolka, R. Turner, and J. Yanus, *Am. Chem. Soc., Org. Coatings Plastic Chem.*, 1978, **38**, 534.

[6] H. W. Gibson and F. C. Bailey, *J. Polym. Sci., Polym. Chem. Ed.*, 1974, **12**, 2141; 1976, **14**, 1661.

[7] J. E. Kuder, J. M. Pochan, S. R. Turner, and D. F. Hinman, *J. Electrochem. Soc.*, 1978, **125**, 1750.

[8] G. Pfister, S. Grammatica, and J. Mort, *Phys. Rev. Lett.*, 1976, **37**, 1360.

[9] D. W. Van Krevelen, ' Properties of Polymers ', Elsevier, New York, 1976, 2nd. edn. p. 384.

[10] For data see L. Doub and J. M. Vandenbelt, *J. Am. Chem. Soc.*, 1947, **69**, 2174; C. N. R. Rao, *Chem. Ind.* (*London*), 1957, 1239; J. R. Dyer, ' Applications of Absorption Spectroscopy of Organic Compounds ', Prentice-Hall, Englewood Cliffs, 1965, p. 18; R. O. Loutfy and R. O. Loutfy, *Can. J. Chem.*, 1976, **54**,1454. For discussion see the last reference and A. R. Katritzky and R. D. Topsom, ' Advances in Linear Free Energy Relationships ', eds. N. B. Chapman and J. Shorter, Plenum Press, New York, 1972, pp. 119—141.

[11] O. Exner in ' Advances in Linear Free Energy Relationships ', eds. N. B. Chapman and J. Shorter, Plenum Press, New York, 1972, p. 32.

[12] J. E. Kuder, H. W. Gibson, and D. Wychick, *J. Org. Chem.*, 1975, **40**, 875.

[13] J. F. Ambrose and R. F. Nelson, *J. Electrochem. Soc.*, 1968, **115**, 1159.

[14] S. C. Creason, J. Wheeler, and R. F. Nelson, *J. Org. Chem.*, 1972, **37**, 4440.

[15] S. Yoshimoto, K. Okamoto, H. Hirata, S. Kusaboyashi, and H. Mikawa, *Bull. Chem. Soc. Jpn.*, 1973, **46**, 358; J. J. O'Malley, J. F. Yanus, and J. M. Pearson, *Macromolecules*, 1972, **5**, 158; W. W. Limburg, U.S.P. 3,884,689/1975.

[16] D. J. Williams, *Macromolecules*, 1970, **3**, 602; W. W. Limburg and D. J. Williams, *ibid.*, 1973, **6**, 787.